Invited paper

Analysis of propagation of orthogonally polarized supermode in straight and curved multicore microstructured fibres

Igor A. Goncharenko and Marian Marciniak

Abstract—We analyze the dependence of radiation loss, effective indices and difference of the effective indices of the two modes with similar field distribution propagating in dual-core microstructured fibres as well as their polarization behavior on fibre parameters (air hole diameter, hole separation, distance between guiding cores) and fibre bending. Optimization of the parameters of such fibres using as vector bend sensors is considered.

Keywords— multicore fibre, microstructured fibre, supermode, birefringence, mode dispersion, method of lines.

1. Introduction

Microstructured or holey fibres are single material fibres with a periodic array of air holes running along the length of the fibre [1, 2]. These fibres guide the light due to a defect (or defects) in the array using two different mechanisms: a photonic band-gap effect or an effective index difference between the defect region, which forms the core, and remainder of the periodic region, which acts as the cladding. Microstructured fibres (MFs) offer exciting new possibilities for guiding of light. They have enormous potential in admitting exotic microstructures with relative ease of manufacturing and can also be made single-mode over a wide range of wavelengths. For many applications, two or more guiding cores rather than just one are required. Examples of such applications include switching, vector bend sensors, phase-locked high-power lasers, fibre couplers and polarization splitters [3–5]. An interesting feature of multicore microstructured fibres (MCMFs) is the possibility to control and modify the shape of their modes by varying the diameter of air holes, hole separation, distance between guiding cores and fibre bends [5, 6].

In a dual-core MF shown in Fig. 1, two supermodes with similar field distribution but different propagation constants and confinement losses propagate equally in both cores [6]. The difference between parameters of both modes is dependent on the structure of MCMF. According to the theory of coupled fibres (see, for instance, [7]), one of the supermodes of the dual-core fibre formed by the sum of the fundamental solutions of separate fibres (separate cores) has propagation constant larger than the propagation constant of the separate fibre by the value of coupling coefficient of two cores. This supermode is called even mode. The second (odd) supermode is formed by subtraction of fundamental solutions and has the propagation constant lower then the separate fibre – by value of the coupling coefficient. In addition each mode exists in two polarization states. Because the cross-section of the dual-core MF with usual hexagonal lattice of air holes substantially differs for the x and y directions, it is natural to expect the difference of parameters and field distributions of modes with orthogonal polarizations.

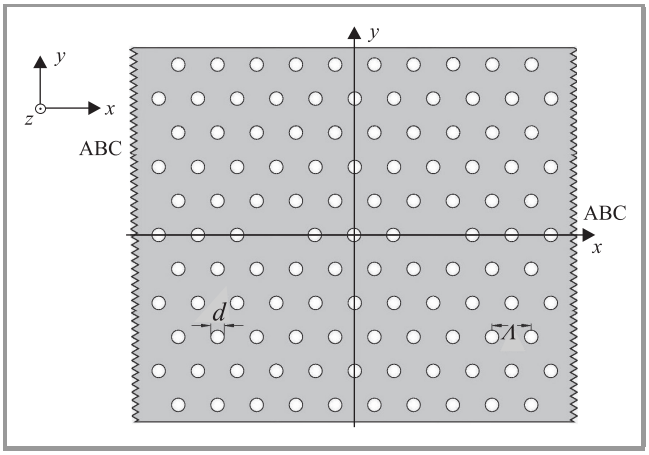

Fig. 1. Cross-section of dual-core microstructured fibre.

In this paper we analyse the mode dispersion in dual-core microstructured fibres in dependence on the MCMF structure and bending. Under the term "mode dispersion" we understand here not the difference of group velocities, but the difference of effective indices and radiation loss coefficients, both of orthogonally polarized modes (polarization mode dispersion or birefringence) and two supermodes of dual-core MF (supermode dispersion).

2. Theory

The cross-section of dual-core MF under investigation with hexagonal lattice is presented in Fig. 1. We use the algorithm based on the method of lines [8, 9] for calculation of mode field distribution, effective refractive indices and radiation loss in MCMF, as we have proven the efficiency of

that method for analysis of single-core MFs [10]. Following the method of lines we divide the structure under investigation into layers in y direction. In each layer the permittivity is assumed to be a function of the x coordinate only: $\varepsilon = \varepsilon(x)$. Wave propagation in z direction is described by $\exp(-jk_z z) = \exp(-j\sqrt{\varepsilon_{re}}\, z)$, ε_{re} being the propagation constant. Therefore, we have $\partial/\partial z = -jk_z = -j\sqrt{\varepsilon_{re}}$. From the Maxwell equations we derive two coupled generalized transmission line equations for the y direction for each layer, which have to be solved [8]:

$$\begin{aligned} \frac{\partial}{\partial \overline{y}} \begin{bmatrix} -\widetilde{H}_x \\ j\widetilde{H}_z \end{bmatrix} &= -\big[R_E\big] \begin{bmatrix} jE_z \\ E_x \end{bmatrix}, \\ \frac{\partial}{\partial \overline{y}} \begin{bmatrix} jE_z \\ E_x \end{bmatrix} &= -\big[R_H\big] \begin{bmatrix} -\widetilde{H}_x \\ j\widetilde{H}_z \end{bmatrix}, \end{aligned} \tag{1}$$

where

$$\begin{aligned} \big[R_E\big] &= \begin{bmatrix} D_{\overline{x}}\mu^{-1}D_{\overline{x}} + \varepsilon_z & -\sqrt{\varepsilon_{re}}D_{\overline{x}}\mu^{-1} \\ -\sqrt{\varepsilon_{re}}\,\mu^{-1}D_{\overline{x}} & \varepsilon_{re}\mu^{-1} - \varepsilon_x \end{bmatrix}, \\ \big[R_H\big] &= \begin{bmatrix} \varepsilon_{re}\,\varepsilon_y^{-1} - \mu & \sqrt{\varepsilon_{re}}\varepsilon_y^{-1}D_{\overline{x}} \\ \sqrt{\varepsilon_{re}}D_{\overline{x}}\varepsilon_y^{-1} & D_{\overline{x}}\varepsilon_y^{-1}D_{\overline{x}} + \mu \end{bmatrix}, \\ E_y &= \varepsilon_y^{-1}\Big[\sqrt{\varepsilon_{re}};\quad -D_{\overline{x}}\Big] \begin{bmatrix} -\widetilde{H}_x \\ j\widetilde{H}_z \end{bmatrix}, \\ \widetilde{H}_y &= \mu^{-1}\Big[D_{\overline{x}};\quad -\sqrt{\varepsilon_{re}}\Big] \begin{bmatrix} jE_z \\ E_x \end{bmatrix}, \end{aligned} \tag{2}$$

$\widetilde{H}_{x,y,z} = \sqrt{\varepsilon_0/\mu_0}\,H_{x,y,z}$, $E_{x,y,z}$ and $H_{x,y,z}$ are the electrical and magnetic field components, $D_{\overline{x}}$ is abbreviation for $\partial/\partial\overline{x}$. All coordinates and dimensions are normalized to the free space wave number k_0 according to $\overline{x} = k_0 x$, $\overline{y} = k_0 y$. The combination of two equations (1) yields wave equations for the electric and magnetic fields, which are completely equivalent

$$\begin{aligned} \frac{\partial^2}{\partial \overline{y}^2} \begin{bmatrix} E_z \\ E_x \end{bmatrix} - \big[R_H\big]\big[R_E\big] \begin{bmatrix} E_z \\ E_x \end{bmatrix} &= 0, \\ \frac{\partial^2}{\partial \overline{y}^2} \begin{bmatrix} -H_x \\ H_z \end{bmatrix} - \big[R_E\big]\big[R_H\big] \begin{bmatrix} -H_x \\ H_z \end{bmatrix} &= 0. \end{aligned} \tag{3}$$

For instance, for the product $[Q_H] = [R_E][R_H]$ we obtain four submatrices:

$$\begin{aligned} Q_{H11} &= -D_{\overline{x}}\mu^{-1}D_{\overline{x}}\mu + \varepsilon_{re}\,\varepsilon_z\,\varepsilon_y^{-1} - \varepsilon_z\mu\,, \\ Q_{H12} &= \sqrt{\varepsilon_{re}}\big(\varepsilon_z\varepsilon_y^{-1}D_{\overline{x}} - D_{\overline{x}}\big)\,, \\ Q_{H21} &= \sqrt{\varepsilon_{re}}\big(D_{\overline{x}} - \varepsilon_x D_{\overline{x}}\varepsilon_y^{-1}\big)\,, \\ Q_{H22} &= -\varepsilon_x D_{\overline{x}}\varepsilon_y^{-1}D_{\overline{x}} + \varepsilon_{re} - \varepsilon_x\mu\,. \end{aligned} \tag{4}$$

The partial differential equations (3) have to be discretized with respect to x coordinate in order to obtain ordinary differential equations, which can be solved analytically. In this case not only the field components but also the permittivities and the radial coordinate x have to be discretized. The discretization has to be done in two different line systems, yielding

$$\begin{aligned} &E_x, H_z, H_y \to \mathbf{E}_x, \mathbf{H}_z, \mathbf{H}_y \qquad H_x, E_z, E_y \to \mathbf{H}_x, \mathbf{E}_z, \mathbf{E}_y \\ &\varepsilon_x \to \boldsymbol{\varepsilon}_x \qquad\qquad \varepsilon_z, \varepsilon_y \to \boldsymbol{\varepsilon}_z, \boldsymbol{\varepsilon}_y \\ &\frac{\partial}{\partial \overline{x}} \to \overline{h}^{-1}\mathbf{D}_x^{\circ} = \overline{\mathbf{D}}_x^{\circ}\,, \qquad \frac{\partial}{\partial \overline{x}} \to \overline{h}^{-1}\mathbf{D}_x^{\bullet} = \overline{\mathbf{D}}_x^{\bullet}\,, \end{aligned} \tag{5}$$

where: $h = k_0 h$ is the normalized discretization distance, $\boldsymbol{\varepsilon}$ are diagonal matrices. The symbols $^{\circ}$ and $^{\bullet}$ indicate the discretization line system to which the quantities belong. In order to take into account the confinement and bend radiation losses, we introduce the absorbing boundary conditions (ABC) [11] on the outer boundaries of the structure.

Now the Eqs. (3) can be rewritten in the form

$$\frac{d^2}{d\overline{y}^2}\,\mathbf{F} - \mathbf{Q}\mathbf{F} = \mathbf{0}\,, \tag{6}$$

where $\mathbf{F} = \mathbf{E}$, $\mathbf{H}$; $\mathbf{E} = \begin{bmatrix} j\mathbf{E}_z \\ \mathbf{E}_x \end{bmatrix}$, $\mathbf{H} = \begin{bmatrix} \mathbf{H}_x \\ j\mathbf{H}_z \end{bmatrix}$ and, for instance,

$$\begin{aligned} Q_{H11} &= -\overline{\mathbf{D}}_x^{\circ}\overline{\mathbf{D}}_x^{\bullet} + \varepsilon_{re}\,\boldsymbol{\varepsilon}_z\boldsymbol{\varepsilon}_y^{-1} - \boldsymbol{\varepsilon}_z\mu\,, \\ Q_{H12} &= \sqrt{\varepsilon_{re}}\big(\boldsymbol{\varepsilon}_z\boldsymbol{\varepsilon}_y^{-1}\overline{\mathbf{D}}_x^{\circ} - \overline{\mathbf{D}}_x^{\circ}\big)\,, \\ Q_{H21} &= \sqrt{\varepsilon_{re}}\big(\overline{\mathbf{D}}_x^{\bullet} - \boldsymbol{\varepsilon}_x\overline{\mathbf{D}}_x^{\bullet}\boldsymbol{\varepsilon}_y^{-1}\big)\,, \\ Q_{H22} &= -\boldsymbol{\varepsilon}_x\overline{\mathbf{D}}_x^{\bullet}\boldsymbol{\varepsilon}_y^{-1}\overline{\mathbf{D}}_x^{\circ} + \varepsilon_{re} - \boldsymbol{\varepsilon}_x\mu\,. \end{aligned}$$

By transformation to main axes (diagonalization)

$$\mathbf{T}_H^{-1}\mathbf{Q}_H\mathbf{T}_H = \boldsymbol{\Gamma}^2, \quad \mathbf{T}_E = j\mathbf{R}_H\mathbf{T}_H\boldsymbol{\Gamma}^{-1}\,,$$

or

$$\begin{aligned} &\mathbf{T}_E^{-1}\mathbf{Q}_E\mathbf{T}_E = \boldsymbol{\Gamma}^2\,, \quad \mathbf{T}_H = j\mathbf{R}_E\mathbf{T}_E\boldsymbol{\Gamma}^{-1}\,, \\ &\mathbf{E} = \mathbf{T}_E\overline{\mathbf{E}}, \quad \mathbf{H} = \mathbf{T}_H\overline{\mathbf{H}} \end{aligned} \tag{7}$$

we obtain uncoupled equations in the transformed domain

$$\frac{d^2}{d\overline{y}^2}\,\overline{\mathbf{F}} - \boldsymbol{\Gamma}^2\overline{\mathbf{F}} = \mathbf{0} \tag{8}$$

with the general solution

$$\overline{\mathbf{F}} = \exp(-\boldsymbol{\Gamma}\overline{y})\,\overline{\mathbf{F}}^{f} + \exp(\boldsymbol{\Gamma}\overline{y})\,\overline{\mathbf{F}}^{b}\,. \tag{9}$$

By solving the eigenvalue problem in Eqs. (7) we obtain the transformation matrices $\mathbf{T}_{E,H}$ and eigenvectors $\boldsymbol{\Gamma}$ for each layer of the structure. In order to obtain the relation between fields at the layer boundaries at the planes $y = y_0$ and $y = y_0 + d$ we introduce a reflection coefficient $\mathbf{r}$ as

the ratio between the backward and forward propagating waves [9]

$$\overline{\mathbf{F}}^{b}(\overline{y}) = \mathbf{r}(\overline{y})\,\overline{\mathbf{F}}^{f}. \tag{10}$$

Inside the layer, the fields and reflection coefficient vary in accordance with

$$\begin{aligned} \overline{\mathbf{F}}^{f}(\overline{y}_0 + \overline{d}) &= \exp(-\boldsymbol{\Gamma}\overline{d})\,\overline{\mathbf{F}}^{f}(\overline{y}_o), \\ \overline{\mathbf{F}}^{b}(\overline{y}_0) &= \exp(-\boldsymbol{\Gamma}\overline{d})\,\overline{\mathbf{F}}^{b}(\overline{y}_0 + \overline{d}), \end{aligned} \tag{11}$$

$$\mathbf{r}(\overline{y}) = \exp(-\boldsymbol{\Gamma}\overline{d})\,\mathbf{r}(\overline{y}_0 + \overline{d})\exp(-\boldsymbol{\Gamma}\overline{d}). \tag{12}$$

where $\overline{d} = k_0 d$, d is the layer thickness.

The transformation of the reflection coefficient at the boundary between two layers II and I, where field components match in original domain (Fig. 2) can be done by using

$$\mathbf{p}_{\mathrm{II}} = (\mathbf{e}_{\mathrm{II}} - \mathbf{h}_{\mathrm{II}})(\mathbf{e}_{\mathrm{II}} + \mathbf{h}_{\mathrm{II}})^{-1} \tag{13}$$

with

$$\begin{aligned} \mathbf{e}_{\mathrm{II}} &= \left(\mathbf{T}_E^{\mathrm{I}}\right)^{-1}\mathbf{T}_E^{\mathrm{II}}(\mathbf{I} + \mathbf{p}_{\mathrm{II}}), \\ \mathbf{h}_{\mathrm{II}} &= \left(\mathbf{T}_H^{\mathrm{I}}\right)^{-1}\mathbf{T}_H^{\mathrm{II}}(\mathbf{I} - \mathbf{p}_{\mathrm{II}}), \end{aligned} \tag{14}$$

where $\mathbf{I}$ stands for the identity matrix.

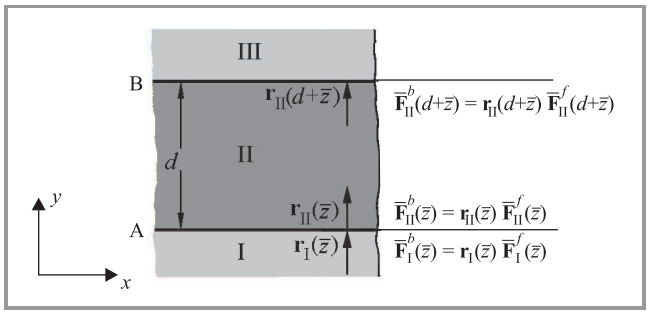

Fig. 2. Transformation of the reflection coefficient between two homogeneous layers.

Using this algorithm we successively transform the reflection coefficient from the top and bottom layers of the structure (where we have $\mathbf{r} = 0$) to a matching plane, which we place in the middle of the central layer (Fig. 3). Taking into account the direction of modes and assuming the symmetry of the structure with respect to the matching plane ($\mathbf{r}_l = \mathbf{r}_u = \mathbf{r}$), we obtain a system of equations:

$$\left[\mathbf{I} - \mathbf{r}^2(\varepsilon_{re})\right]\overline{\mathbf{F}}^{f} = \mathbf{0}, \tag{15}$$

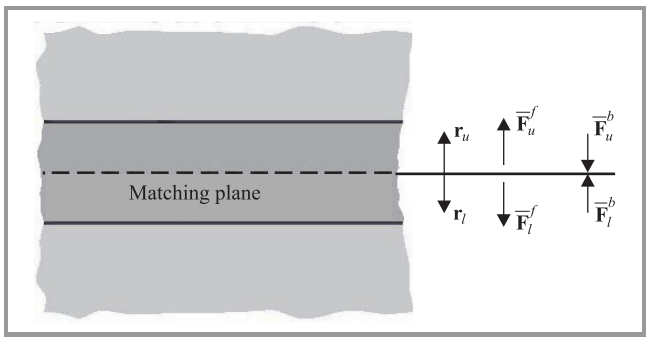

Fig. 3. Transformation of the reflection coefficient from the top and bottom to a matching plane.

from which the determinant equation

$$\det\left[\mathbf{I} - \mathbf{r}^2(\varepsilon_{re})\right] = \det\left[\mathbf{I} - \mathbf{r}(\varepsilon_{re})\right]\cdot\det\left[\mathbf{I} + \mathbf{r}(\varepsilon_{re})\right] = \mathbf{0} \tag{16}$$

can be derived. The solution of the determinant equation gives us the propagation constant ε_{re}, which is complex because of the radiation. The real part of the $\sqrt{\varepsilon_{re}}$ is the effective refractive index n_{eff}, while the imaginary one stands for the radiation loss coefficient $\alpha = 0.0868 \cdot \mathrm{Im}\left(\sqrt{\varepsilon_{re}}\right)$ dB/cm.

After determining ε_{re}, we can compute the modes in the matching plane, and consequently the field distribution in the whole structure.

The expression (16) is a quadratic equation and has two solutions. One of the solutions follows from the first factor $\det\left[\mathbf{I} - \mathbf{r}(\varepsilon_{re})\right]$ of the equation and corresponds to the x-polarized mode. Another root obtained from the second factor $\det\left[\mathbf{I} + \mathbf{r}(\varepsilon_{re})\right]$ describes the mode polarized in orthogonal y direction.

3. Results and discussion

3.1. Birefringence and supermode dispersion in straight MCMFs

We have applied the algorithm described above to calculate mode field distribution, propagation constants and radiation loss coefficients for dual-core MFs. The results are plotted in Figs. 4–7.

Figure 4 shows the electric field transverse component distribution of the orthogonally polarized odd and even modes in MF with two guiding cores separated by three air holes. The air hole diameter d of the MF equals to 0.64 μm in that case; the ratio of hole diameter to hole separation d/Λ is 0.2 and the wavelength of propagating radiation is 1.5 μm. The first ten and last five contour lines in the figure are spaced by 0.01 of the field maximum value, while others are spaced by 0.025. As one can see from the figure, the field distributions of modes of both polarizations look quite similar in high intensity region and slightly differ for low intensities nearby the fibre boundaries. This is because the MF structure is anisotropic in the cross-section. The same "slight but significant difference" in the field profiles of x- and y-polarized modes has been reported in [12]. The field distributions for odd and even supermodes are also similar for high intensity region, but even modes have additional low intensity components between cores.

Figures 5 and 6 show, respectively, the effective indices and the difference between effective indices of even and odd modes of dual-core MF and the orthogonal polarization states of these modes as a function of the ratio d/Λ

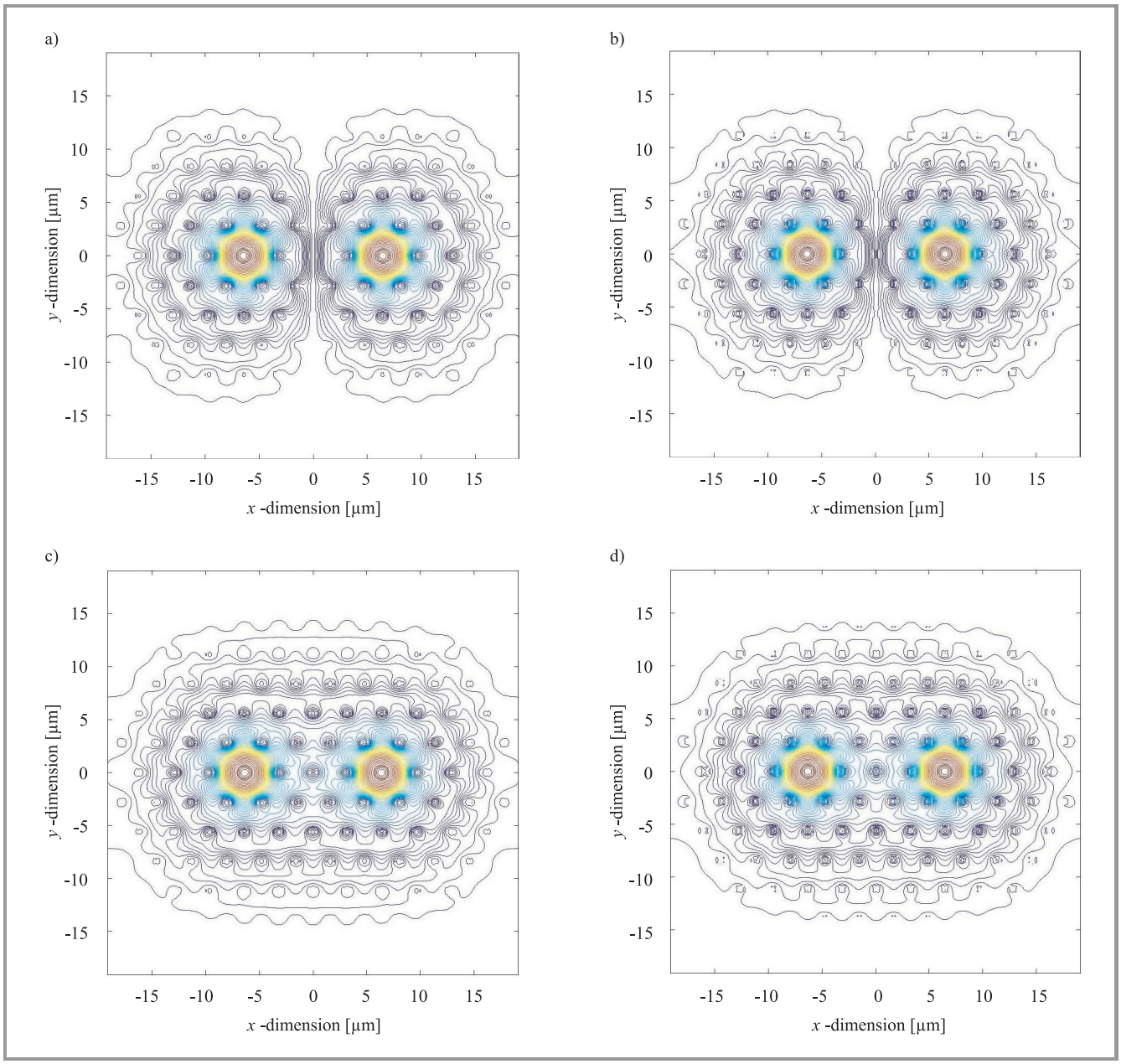

Fig. 4. Transverse electric field distribution of the orthogonally polarized modes: (a)$|E_x(x, y)|$ for x-polarized odd mode; (b) $|E_y(x, y)|$ for y-polarized odd mode; (c) $|E_x(x, y)|$ for x-polarized even mode; (d) $|E_y(x, y)|$ for y-polarized even mode.

for MF with 3 holes between cores and radiation wavelength $\lambda = 1.5$ μm (a), function of the number of holes between guiding cores (core separation) for $d/\Lambda = 0.2$ and $\lambda = 1.5$ μm (b), and function of normalized wavelength λ/Λ for $d/\Lambda = 0.2$ and 3 holes between cores (c). Plots for the effective indices of different MCMF supermodes on Fig. 5c coincide within printing resolution.

Figure 7 shows similar dependences for the radiation loss of the two modes in both polarization states. In Fig. 6, curves *1–4* present, respectively, the birefringence of the odd $n^x_{ef\,od} - n^y_{ef\,od}$ (curve *1*) and even $n^x_{ef\ ev} - n^y_{ef\,ev}$ (curve *2*) modes and supermode dispersion for x-polarized $n^x_{ef\,ev} - n^x_{ef\,od}$ (curve *3*) and y-polarized $n^y_{ef\,ev} - n^y_{ef\,od}$ (curve *4*) modes. In Figs. 5 and 7, the effective indices and radiation loss coefficient α are plotted: solid lines correspond to x-polarized modes and dashed lines represent y-polarized modes. Curves *1* and *2* describe effective indices and loss of the odd and even supermodes, respectively. In these calculations we take into account the dependence of the material refractive index on wavelength, using the Sellmeier equation.

As one can see, the effective indices of the all supermodes decrease with enlarging fibre air-filling fraction or reducing the radiation wavelength. As the core separation increases the effective indices of the orthogonally polarized odd and even supermodes correspondingly decrease and increase, approaching effective indices of the x- and y-polarized modes of the single-core MF. The difference

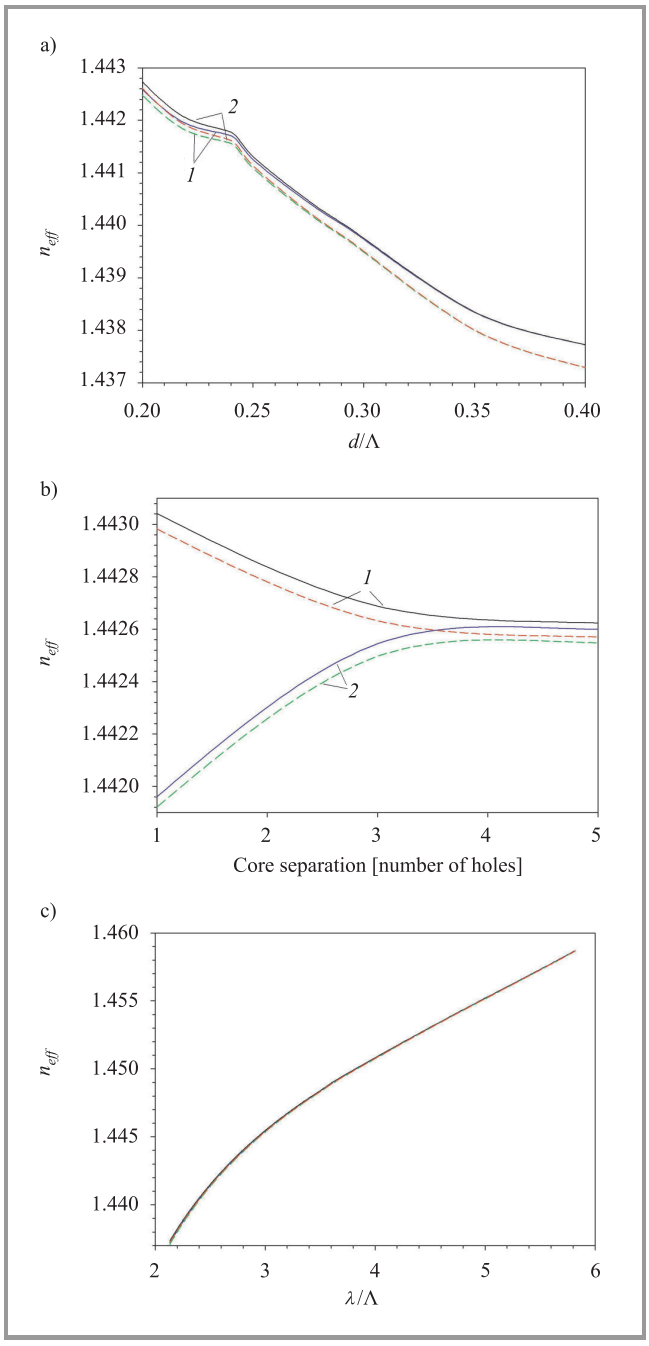

Fig. 5. Effective indices of the supermodes of dual-core MF as a function of (a) the ratio d/Λ; (b) core separation; (c) normalized wavelength λ/Λ. Solid and dashed lines correspond to the *x*- and the *y*-polarized modes. Curves *1* and *2* describe the effective indices of the odd and even supermode, respectively.

between effective indices of orthogonally polarized modes increases with enlarging the hole diameter or reducing hole separation. At the same time, the polarization birefringence has more flat dependence on the separation of fibre cores. With increasing core separation, birefringence of the odd and even supermodes decreases and increases correspondingly, converging to the birefringence value of the mode propagated in a single-core microstructured fibre with similar parameters (dashed line in Fig. 6b).

Similar small influence of microstructured fibre core separation on polarization beat length has been observed experimentally by the group of dr. J. Wojcik from the Lublin Maria Curie-Sklodowska University (UMCS) [13]. Increase of fibre air-filling fraction d/Λ or core separation leads to reduction the difference between effective indices of the odd and even modes of dual-core MF. For $d/\Lambda \geq 0.4$ (for $\lambda = 1.5$ μm) and/or separation of the cores in more than 5 holes, the effective indices of the both modes prac-

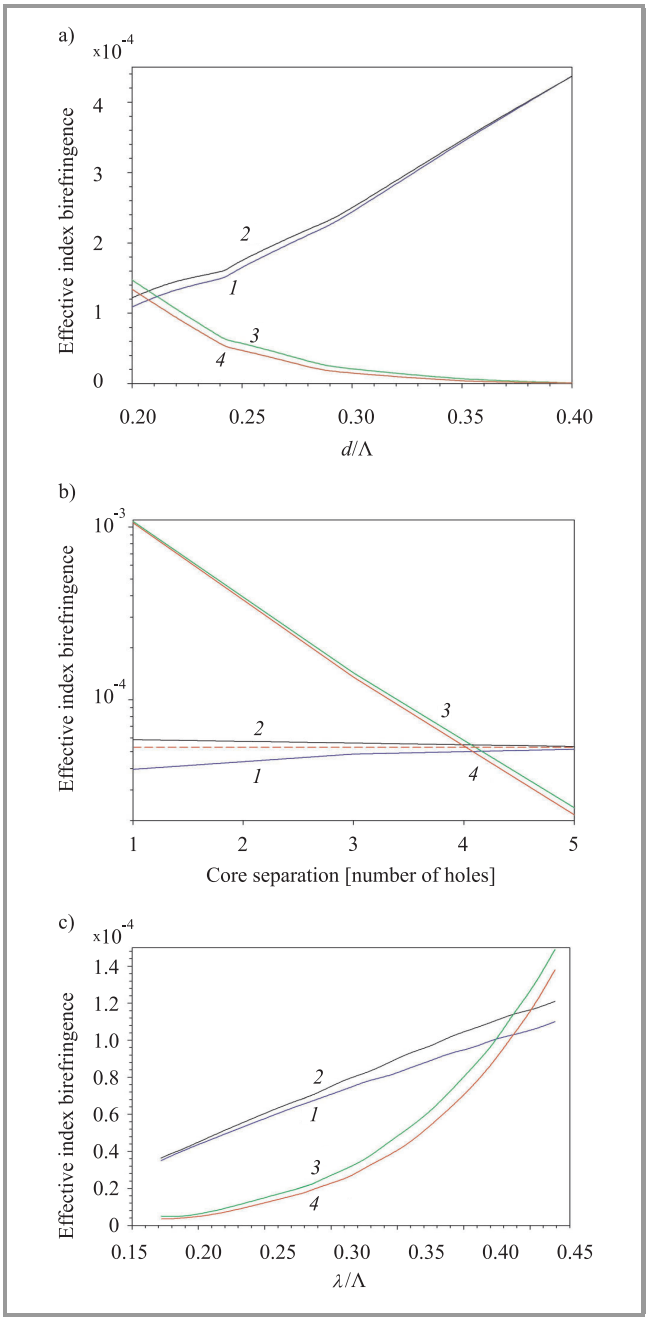

Fig. 6. Effective index birefringence and supermode dispersion of dual-core MF as a function of (a) the ratio d/Λ; (b) core separation; (c) normalized wavelength λ/Λ. The plot numbers indicate $n^x_{ef\,od} - n^y_{ef\,od}$ (*1*), $n^x_{ef\,ev} - n^y_{ef\,ev}$ (*2*), $n^x_{ef\,ev} - n^x_{ef\,od}$ (*3*), and $n^y_{ef\,ev} - n^y_{ef\,od}$ (*4*). Dashed line in (b) describes polarization birefringence of a single-core microstructured fibre.

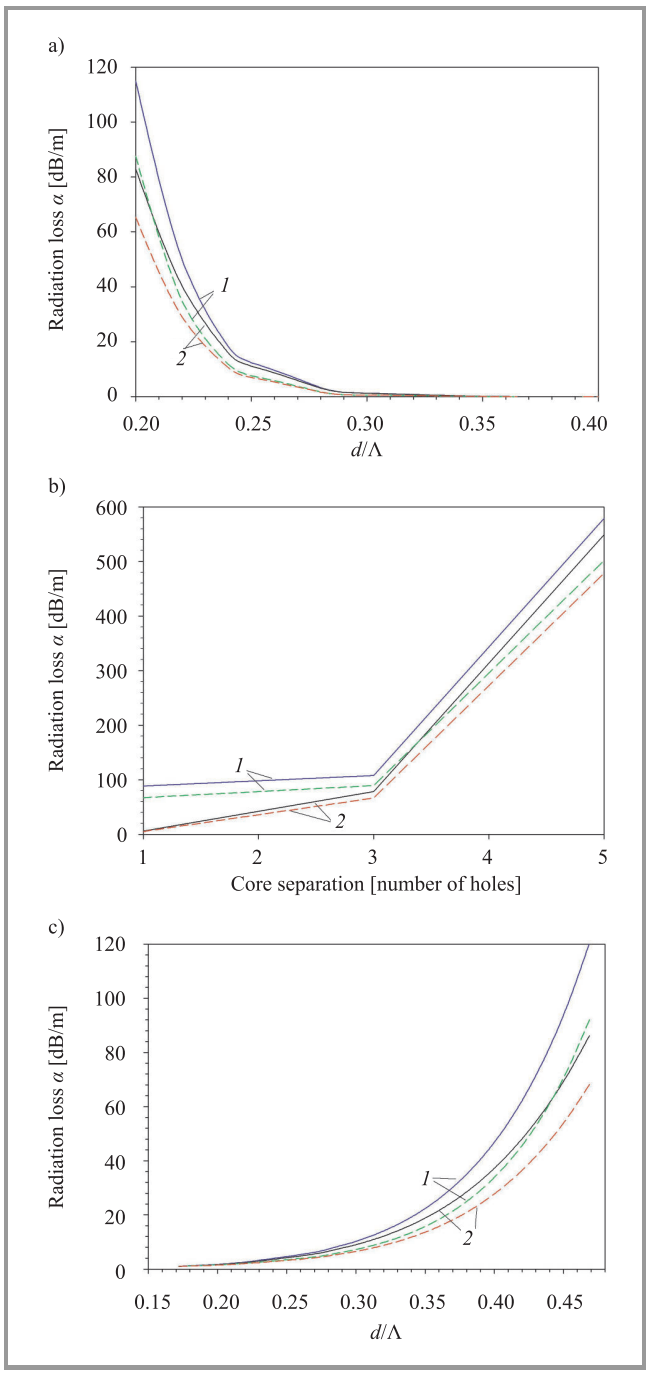

Fig. 7. Radiation loss coefficient of the modes of dual-core MF as a function of (a) the ratio d/Λ; (b) core separation; (c) normalized wavelength λ/Λ.

tically coincide. Thus, there is no coupling between cores and each core behaves as a separate fibre. Both supermode dispersion and polarization birefringence are reduced with decrease of radiation wavelength.

In such case, the difference between orthogonally polarized modes drops approximately linearly with decrease of wavelength, while the difference between even and odd modes has more sharp exponential wavelength dependence. In the short wavelength region ($\lambda/\Lambda \leq 0.18$ for $d/\Lambda = 0.2$) the difference between effective indices of even and odd modes is negligible and two cores are practically decoupled. Increasing the ratio d/Λ or decreasing core separation reduces the radiation loss in MCMFs. At that, the loss of *y*-polarized modes is lower, because the fields of these modes decay steeper to the fibre boundaries. Calculations of the influence of core separation have been done for fibres of identical size. Thus, the extension of distance between cores leads to reduction of distance from the cores to fibre outer boundaries (cladding thickness). As a result, the decay of mode field amplitudes on the fibre boundaries is insufficient; this explains the rise of calculated radiation loss for large core separation.

In calculation of MFs with some ratios d/Λ the *calculated* fibre dimension, which is an integer multiply of the discretization step, slightly differs from the *real* fibre dimension. This can explain the small kinks observed on the curves in Figs. 5a, 6a and 7a.

3.2. Curved dual-core MFs

Microstructured fibres being used, for instance, in communication lines can be subject to bending. Sensitivity to bends is also important issue for multicore MFs used as bend sensors and couplers. Therefore, the behavior of multicore MFs modes in bend region has to be investigated. For straight MF we used the Cartesian coordinate system whereas the cylindrical coordinate system where the angular coordinate φ corresponds to the bend is used for curved MF [6].

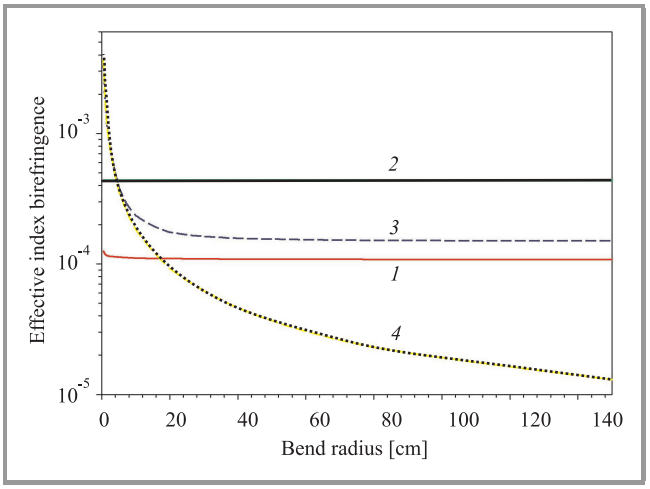

Fig. 8. Birefringence and supermode dispersion of the MF as a function of bend radius.

Figure 8 shows birefringence ($n^x_{ef\,od} - n^y_{ef\,od}$, solid lines *1* and *2*) and supermode dispersion ($n^x_{ef\,ev} - n^x_{ef\,od}$, dashed lines *3* and *4*) of the MF as a function of bend radius for different cores separation and air-filling fraction. Curves *1* and *3* correspond to MFs with $d/\Lambda = 0.2$ and curves *2* and *4* relate to $d/\Lambda = 0.4$. As one can see from plots *1* and *2*, the difference between effective indices of orthogonally polarized modes doesn't change with the bend. In opposite, the difference between effective indices of odd

and even supermodes increases with reducing bend radius. The supermode dispersion of the MCMFs with larger ratio d/Λ more sharply depends on the fibre bend.

Bending causes redistribution of optical power of two modes of dual-core MF between the cores and eliminates the first and second modes quasi-degeneracy. The power of the odd modes is concentrated mostly in the core on the inner side of the bend, and amplitude of the mode in outer core decreases [6]. The even mode field concentrates mostly in the outer core. The difference between mode amplitudes in left and right cores in dual-core MFs increases as the bend radius decreases (see Fig. 9). Thus, by comparing

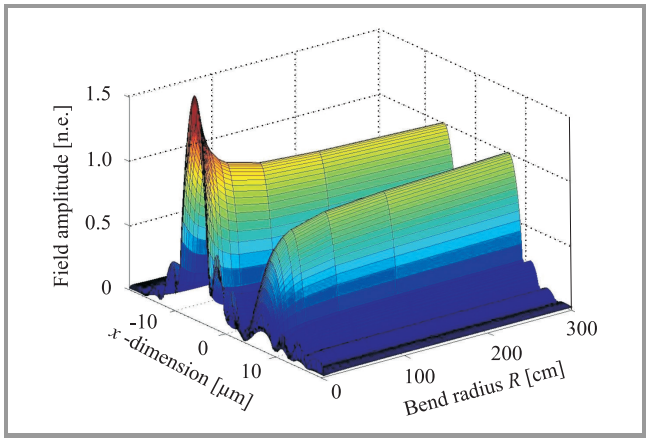

Fig. 9. Variation of the odd mode amplitude in both cores of the dual-core MF with the fibre bend radius.

the measured power in both cores of the MF it is possible to determine the value of fibre bend radius. Change of bend direction leads to opposite distribution of the mode fields. This feature allows using the dual-core MFs as vector bend sensors, i.e., sensors for determining both the bend value and direction.

4. Conclusions

We have calculated the field distribution, effective indices and radiation loss of two supermodes in both polarization states propagating in dual-core microstructured fibres with different parameters and analyzed the birefringence and supermode dispersion as a function of fibre parameters, wavelength and bend. This analyzis shows that the effective indices of the MCMF supermodes decrease with enlarging fibre air-filling fraction or reducing the radiation wavelength. As the core separation increases, the effective indices of the orthogonally polarized odd and even supermodes decrease and increase correspondingly and approach the values of effective indices of the x- and y-polarized modes of the single-core MF. The birefringence increases with enlarging the hole diameter, wavelength or reducing hole separation. The polarization birefringence exhibits more flat dependence on the separation of fibre cores. With increasing core separation the birefringence of the odd supermode slightly decreases and the one of the even mode increases; both tend to the birefringence of the mode of single-core fibre with similar parameters – from different sides. The supermode dispersion reduces with increasing fibre air-filling fraction, core separation or decreasing wavelength. For $d/\Lambda \geq 0.4$ (for $\lambda = 1.5$ μm) and/or separation of the cores in more than 5 holes the effective indices of the both supermodes practically coincide and each core behaves as a separate fibre. The same core decoupling is achieved for propagating radiation with short wavelength.

Fibre bending causes redistribution of optical power of two supermodes of dual-core MF between the cores. The power of the odd mode is concentrated mostly in the core, which is on inner side of the bend, and amplitude of the mode in the outer core decreases. The even mode concentrates mostly in outer core. The difference between mode amplitudes in both cores in dual-core MFs increases with reduction of the bend radius. At that, bending doesn't change the polarization birefringence. In opposite, the supermode dispersion increases as the bend radius reduces.

Acknowledgements

Igor A. Goncharenko thanks the Belarussian Fund of Fundamental Research for the financial support of this work. The authors thank the European Project COST Action P11 "Physics of linear, nonlinear and active photonic crystals" for stimulating interactions.

References

[1] J. C. Knight, J. Broeng, T. A. Birks, and P. St. J. Russell, "Photonic bandgap guidance in optical fibers", *Science*, vol. 282, pp. 1476–1478, 1998.

[2] T. M. Monro, D. J. Richardson, N. G. R. Broderick, and P. J. Bennet, "Holey optical fibers: an efficient modal model", *J. Lightw. Technol.*, vol. 17, pp. 1093–1102, 1999.

[3] P. J. Roberts and T. J. Shepherd, "The guidance properties of multicore photonic crystal fibres", *J. Opt. A.: Pure Appl. Opt.*, vol. 3, pp. S133–S140, 2001.

[4] L. Zhang and C. Yang, "A novel polarization splitter based on the photonic crystal fiber with nonidentical dual cores", *IEEE Photon. Technol. Lett.*, vol. 16, pp.1670–1672, 2004.

[5] A. Mafi and J. V. Moloney, "Shaping modes in multicore photonic crystal fibers", *IEEE Photon. Technol. Lett.*, vol. 17, pp. 348–350, 2005.

[6] I. A. Goncharenko, "Propagation constants and radiation loss of the modes in curved multi-core microstructure fibres", in *Proc. ICTON 2004*, Wrocław, Poland, 2004, vol. 2, pp. 107–110.

[7] A. W. Snyder and J. D. Love, *Optical Waveguide Theory*. London-N.Y.: Chapman and Hall, 1983.

[8] R. Pregla, "The method of lines as generalized transmission line technique for the analysis of multilayered structures", *Int. J. Electron. Commun. (AEÜ)*, vol. 50, pp. 293–300, 1996.

[9] S. F. Helfert and R. Pregla, "The method of lines: a versatile tool for the analysis of waveguide structures", *Electromagnetics*, vol. 22, pp. 615–637, 2002.

[10] I. A. Goncharenko, S. F. Helfert, and R. Pregla, "Radiation loss and mode field distribution in curved holey fibers", *Int. J. Electron. Commun. (AEÜ)*, vol. 59, pp. 185–191, 2005.

[11] R. Pregla, "MoL-BPM method of lines based beam propagation method", in *Methods for Modelling and Simulation of Guided-Wave Optoelectronic Devices*, Ed. W. P. Huang. Cambridge: EMW Publishing, 1995, pp. 65–70.

[12] F. Fogli, L. Saccomandi, P. Bassi, G. Bellanca, and S. Trillo, "Full vectorial BPM modeling of index-guiding photonic crystal fibers and couplers", *Opt. Expr.*, vol. 10, pp. 54–59, 2002.

[13] Private communication by dr. Jan Wojcik.

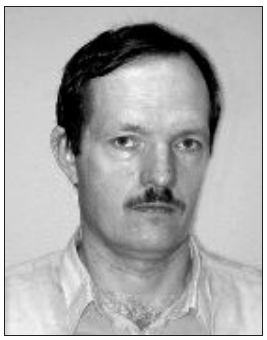

Igor A. Goncharenko graduated from the Physics Department of the Belarussian State University in 1981. He received the Ph.D. degree in physics and mathematics from the USSR Academy of Sciences (Moscow) in 1985 and Dr.Sci. degree from the National Academy of Sciences of Belarus (Minsk) in 2001. From 1985 until August 2007 he worked in Institute of Electronics of the National Academy of Sciences of Belarus. Last time he took up the positions of Chief Research Fellow at the Institute. In 1994 he was awarded a Royal Society Fellowship and worked with the Optoelectronics Research Centre, University of Southampton, UK. In 1996 he was awarded the Alexander von Humboldt Research Fellowship and carried out research at the FernUniversitaet in Hagen, Germany. In 2007 he carried out the analysis of waveguiding conditions in liquid crystal and investigated photonics switches on the base of LC waveguides in Hong Kong University of Science and Technology. Since September 2007 Dr. Goncharenko takes up the position of Professor of the Department of Natural Sciences in the Institute for Command Engineers of the Ministry of Emergencies of the Republic of Belarus. Also he has a part time Professor position in Belarussian National Technical University, department of laser technique and technology, where he gives special courses of lectures "Wave optics" and "Physical optics". At the same time he gives special course of lectures "Fibre optics" for students of Physics Department of Belarussian State University. His present scientific interests include the theory of optical fibres, microstructure (photonic crystal) fibres, active and passive fibre devices, tuneable fibre and waveguide lasers and amplifiers, multilayer waveguide structures, pulse propagation and nonlinear effects in optical fibres, optical information processing, optics logic elements and so on. He has contributed to a number of national and international conferences and published more than 180 papers in scientific journals including 38 patents. Doctor Goncharenko is a member of the IEEE. He participates in Program Committees of the *WSEAS International Conference on Global Optical & Wireless Network*, *SPIE Europe International Congress on Optics & Optoelectronics*, *Conference on Photonic Crystal & Fibers* and *International Conference for Young Scientists on Optics*. He serves as a reviewer for several international scientific journals. His biography has been cited in Marquis *Who's Who in Science and Engineering*, *Who's Who in America* and in the International Biographical Centre, Cambridge *2000 Outstanding Scientists of the 21st Century, Living Science Award* and *21st Century Awards for Achievement*.

e-mail: Igor02@tut.by
Institute for Command Engineers
of the Ministry of Emergencies of the Republic of Belarus
Department of Natural Sciences
25 Mashinostroiteley Str.
220118 Minsk, Belarus

Marian Marciniak Associate Professor has been graduated in solid state physics from Marie-Curie Sklodovska University in Lublin, Poland, in 1977. From 1985 to 1989 he performed Ph.D. studies in electromagnetic wave theory at the Institute of Fundamental Technological Research, Polish Academy of Sciences, followed linebreak by Ph.D. degree (with distinction) in optoelectronics received from Military University of Technology in Warsaw. In 1997 he received his Doctor of Sciences (habilitation) degree in physics/optics from Warsaw University of Technology. From 1978 to 1997 he held an academic position in the Military Academy of Telecommunications in Zegrze, Poland. In 1996 he joined the National Institute of Telecommunications in Warsaw, where he actually leads the Department of Transmission and Fibre Technology. Previous activities have included extended studies of optical waveguiding linear and nonlinear phenomena with analytic and numerical methods including beam-propagation methods. Actual research interests include photonic crystal technology and phenomena, optical packet-switched networks, and the future global optical and wireless network. Recently he has introduced and developed a concept of a hybrid real-time service end photonic packet network. He is an author or co-author of over 200 technical publications, including a number of conference invited presentations and 14 books authored, co-authored and/or edited by himself. He is a Senior Member of the IEEE – Lasers & Electro-Optics, Communications, and Computer Societies, a member of The New York Academy of Sciences, The Optical Society of America, SPIE – The International Society for Optical Engineering and its Technical Group on Optical Networks, and of the American Association for the Advancement of Science. In early 2001 he originated the IEEE/LEOS Poland Chapter and he has served as the Chairman of that Chapter until July 2003. He is widely involved in the European research for optical telecommunication networks, systems and devices. He was the originator of accession of Poland to European Research Programs in the optical telecommunications domain, in

chronological order: COST 240 *Modelling and Measuring of Advanced Photonic Telecommunication Components*, COST P2 *Applications of Nonlinear Optical Phenomena*, COST 266 *Advanced Infrastructure for Photonic Networks*, COST 268 *Wavelength-Scale Photonic Components for Telecommunications*, COST 270 *Reliability of Optical Components and Devices in Communications Systems and Networks*, COST 273 *Towards Mobile Broadband Multimedia Networks*, and very recently two new starting actions COST 288 *Nanoscale and Ultrafast Photonics* and COST P11 *Physics of Linear, Nonlinear and Active Photonic Crystals*. In all but two those projects he acted as one of the originators at the European level. He has been appointed to Management Committees of all those Projects as the Delegate of Poland. In addition, he has been appointed as the Evaluator of the European Union's 5th Framework Program proposals in the Action Line *All-Optical and Terabit Networks* and 6th FP *Research Networking Test-beds*. He is a Delegate to the International Telecommunication Union, Study Group 15: *Optical and Other Transport Networks*, and to the International Electrotechnical Commission, Technical Committee 86 *Fibre Optics* and its two sub-Committees. He served as a member of Polish Delegation to the World Telecommunication Standards Assembly WTSA 2000. From 2002 he participates in the work of the URSI – *International Union of Radio Science, Commission D – Electronics and Photonics*. In 2000 he originated and actually serves as the Chairman of the Technical Committee 282 on *Fibre Optics* of the National Committee for Standardisation. Since May 2003 he serves as the Vice-President of the Delegation of Poland to the Intergovernmental Ukrainian-Polish Working Group for Cooperation in Telecommunications. He is the originator and the main organiser of the *International Conference on Transparent Optical Networks* ICTON starting in 1999, and a co-located events the *European Symposium on Photonic Crystals* ESPC and *Workshop on All-Optical Routing* WAOR since 2002 and *Global Optical and Wireless GOWN Seminar* since 2004. He is the Technical Program Committee Co-Chair of the *International Conference on Advanced Optoelectronics and Lasers* CAOL, and he participates in Program Committees of the *Conference on the Optical Internet & Australian Conference on Optical Fibre Technology* COIN/ACOFT, the *International Conference on Mathematical Methods i*n Electromagnetic *Theory* MMET, the *International Workshop on Laser and Fiber-Optical Network Modeling* LFNM, and the *International School for Young Scientists and Students on Optics, Laser Physics and Biophysics/Workshop on Laser Physics and Photonics*. He serves as a reviewer for several international scientific journals, and he is a Member of the Editorial Board of *Microwave & Optoelectronics Technology Letters* journal, Wiley, USA, and the *Journal of Telecommunications and Information Technology*, National Institute of Telecommunications, Poland. Languages spoken: Polish (native), English, French, and Russian. His biography has been cited in Marquis *Who's Who in the World, Who's Who in Science and Engineering*, and in the *International Directory of Distinguished Leadership of the American Biographical Institute*.

e-mail: M.Marciniak@itl.waw.pl
e-mail: marian.marciniak@ieee.org
Department of Transmission and Fibre Technology
National Institute of Telecommunications
Szachowa st 1
04-894 Warsaw, Poland